PAPER

Current sharing in double-sided REBCO tapes

IOP Publishing Superconductor Science and Technology
Supercond. Sci. Technol. **37** (2024) 075006 (10pp) https://doi.org/10.1088/1361-6668/ad4e76

Current sharing in double-sided REBCO tapes

Shengchen Xue[1], Yi Li[2,3,4], Lingfeng Zhu[2,3,4], Bhabesh Sarangi[2,3,4], Jithin Sai Sandra[2,3,4], Jian Rong[2,3,4], Nghia Mai[1], Siwei Chen[2,3,4], Atik Chavda[2,3,4], Umesh Sambangi[2,3,4], Jithin Peram[2,3,4], Prakash Parthiban[2,3,4] and Venkat Selvamanickam[2,3,4,*]

[1] AMPeers LLC, Houston, TX 77059, United States of America
[2] Department of Mechanical Engineering, University of Houston, Houston, TX 77204, United States of America
[3] Advanced Manufacturing Institute, University of Houston, Houston, TX 77023, United States of America
[4] Texas Center for Superconductivity, University of Houston, Houston, TX 77204, United States of America

E-mail: selva@uh.edu

Received 7 February 2024, revised 10 May 2024
Accepted for publication 21 May 2024
Published 6 June 2024

Abstract

Current sharing between RE–Ba–Cu–O (REBCO, RE = rare earth) tapes within a high-temperature superconducting coil or cable is important to avoid damage from uncontrolled quench of superconducting devices operating at high currents. Current sharing between REBCO tapes is found to be limited by the contact resistivity between adjacent tapes, which is about 20x higher in the REBCO-facing-substrate (face-to-back) configuration that is commonly used in devices compared to a REBCO-facing-REBCO (face-to-face) configuration. Double-sided REBCO tapes always offer face-to-face contacts between adjacent tapes, and this benefit of excellent current sharing has been validated in experiments wherein an artificial defect is introduced in one tape in a 2-ply tape stack. Additionally, current sharing between the two REBCO layers within one double-sided REBCO tape has also been investigated. Slotting of the double-sided tapes, wherein slots through the insulating buffer stack are filled with a conductive material, has been found to significantly enhance the current sharing from one REBCO layer to the opposite layer.

Keywords: double-sided, REBCO, current sharing

1. Introduction

The remarkably superior current densities of RE–Ba–Cu–O (REBCO, RE = rare earth) tapes enable high-power-density and highly efficient electric machines and high magnetic field applications, beyond the capability of low-temperature superconductors (LTSs) [1]. At such high current densities, sustained through a film just 2–5 μm thick, the superconductor is susceptible to localized heating at defective spots that are invariably present in a long tape. Since each tape turn of coils comprising a superconducting device is typically insulated, the hot spots do not dissipate easily which causes a thermal runaway, leading to a catastrophic failure [2]. Hence, the normal zone, i.e. the hot spot, must be detected rapidly to protect the device.

A problem with high temperature superconductors (HTSs) is that the normal zone propagation velocity is much lower (0.01–0.1 m s^{-1}) [3–5] than that of LTSs [6–10]. This results in a slow-spreading normal zone and thus, a slow increase in fault-induced voltage. Simultaneously, the slow spread of heat results in high local temperatures before the voltage increases

* Author to whom any correspondence should be addressed.

sufficiently for external detection. These two effects combined can lead to thermal runaway and catastrophic failure of the coil before quench detection.

This problem has been well recognized, and several methods are being developed for quench detection as well as HTS coil designs have been modified for quench tolerance. These include acoustic emission detection, acoustic thermometry, Rayleigh scattering, quench antennas, ultrasonic wave-based detection, varying laminations, no-insulation coils, different insulation materials, and epoxies. However, each solution has some drawbacks such as susceptibility to vibrations, low signal-to-noise ratio, and extrinsic sensors co-wound with the tape that increase the complexity of coil fabrication or reduce the overall current density.

Uniform, long REBCO tapes with minimal defects are desirable to avoid hot spots that are difficult to detect in use. The critical current (I_c) of long REBCO tapes is universally tested for uniformity only at 77 K in zero applied magnetic field. But there is strong evidence that even tapes that exhibit uniform I_c at 77 K, 0 T can have inconsistent I_c in a magnetic field at lower temperatures [11, 12]. Consequently, sections of a long tape that have lower I_c in a magnetic field at lower temperatures—that are not detected by I_c measurements at 77 K, 0 T—can be a location of quench and onset of failure.

While long tapes with uniform critical current are highly desirable to avoid such hot spots, methods to manage local defects in REBCO tapes have to be investigated. Unlike metallic superconductors like Nb_3Sn which consist of thousands of fine filaments in each strand, the wide geometry of REBCO tapes is not conducive for easy current sharing between tapes in a coil or cable. The objective of this work is to develop defect tolerant REBCO conductors that promote current sharing between tapes to bypass current around local defects to reduce the possibility of uncontrolled quench and potential failure.

Previous research to improve current sharing in REBCO tape stacks/cables has been through techniques to change the inter-strand interface, including cold pressing [13–16], hot pressing [17], ultrasonic welding [18, 19], metal-plating [13, 17], and conductive polymer-CNT coating [20]. However, modification of the architecture of a single REBCO tape has not been explored to improve current sharing. Even in a no-insulation coil with electrically-conductive solder between each turn of tapes in the winding [21], or in a cable with solder-impregnated REBCO tape stacks [22, 23], current sharing between tapes is limited by the insulating oxide buffer layers. In these cases, REBCO-facing-substrate (face-to-back, F2B) or substrate-facing-substrate (back-to-back, B2B) contacts are inevitable, and current sharing requires detour around the insulating oxide buffer layers. So, we have been exploring methods such as fully or partially electrically-conductive buffer layers to reduce contact resistivity. In this manuscript, we report our work on double-sided tapes, which enables inter-tape contact always REBCO-facing-REBCO, i.e. face-to-face (F2F), to reduce contact resistivity and promote current sharing. In addition, we demonstrate an approach to enhance current sharing between the two REBCO layers of a single double-sided tape by partially removing the insulating buffer layers by slotting.

Recently, we reported the development of double-sided REBCO tapes by Advanced metal organic chemical vapor deposition (MOCVD) wherein REBCO films as thick as 3.4 μm in thickness are deposited *simultaneously* on both sides of a tape [24]. Double-sided tapes with approximately 3 μm thick films on each side have been demonstrated with a critical current density of 2.6 MA cm^{-2} at 77 K, self-field, and I_c of 530 A/4 mm at 20 K, 20 T [24]. The use of double-sided tapes enables face-to-face contact, i.e. REBCO films of adjacent tapes facing each other, a configuration with much lower contact resistivity than face-to-back contact, the latter being the configuration in all devices made so far with standard REBCO tapes.

2. Experiments

A standard buffer stack architecture of $LaMnO_3$/homo-epi MgO/Ion beam Assisted Deposition MgO/ Y_2O_3/Al_2O_3 was deposited on both sides of electropolished Hastelloy C276 substrates. The $LaMnO_3$ cap layer of such a buffer stack exhibits an out-of-plane texture of $\sim 2^\circ$ and an in-plane texture of $\sim 6^\circ$ on both sides. (Gd,Y)BCO films with 5% Zr addition were deposited simultaneously in a single step on both sides of 30 cm long substrates with double-sided buffer stack in an Advanced MOCVD reactor [24]. A silver overlayer of ~ 2 μm thickness was deposited on both sides by magnetron sputtering. The I_c of the double-sided REBCO tapes was measured by reel-to-reel scanning hall probe microscopy (SHPM) at 77 K, 0 T [25, 26]. The transport I_c of short sections of these samples were also measured on each of the two sides by the four-probe method. In addition to double-sided tapes, standard single-sided commercial REBCO tapes with ~ 2 μm thick REBCO film were also used in this study for current sharing experiments. The tapes used for current sharing experiments were 4 mm wide, laser slit from 12 mm wide double-sided and single-sided tapes. Copper of 10 μm thickness was electroplated on the laser-slit tapes after silver sputter deposition to seal the edges. To test current sharing from a defective tape to a normal tape in parallel, a 2 mm diameter artificial defect was created by punching hole or laser cutting in one of the tapes. Double-sided tapes were tested for current sharing between the two REBCO layers within one tape itself, where a 2 mm diameter defect was introduced in one of the two layers of the tape. Current sharing between two double-sided tapes was also examined where a 2 mm diameter defect was created in one layer of one of the two tapes.

Current sharing experiments were conducted in a test rig, shown in figure 1. In a 2-ply stack with two single-sided tapes, a tape with an artificial defect and a normal tape (parallel tape) were soldered together, and the REBCO side of the defective tape was in contact with current lead. For testing current sharing between the two REBCO layers within one double-sided

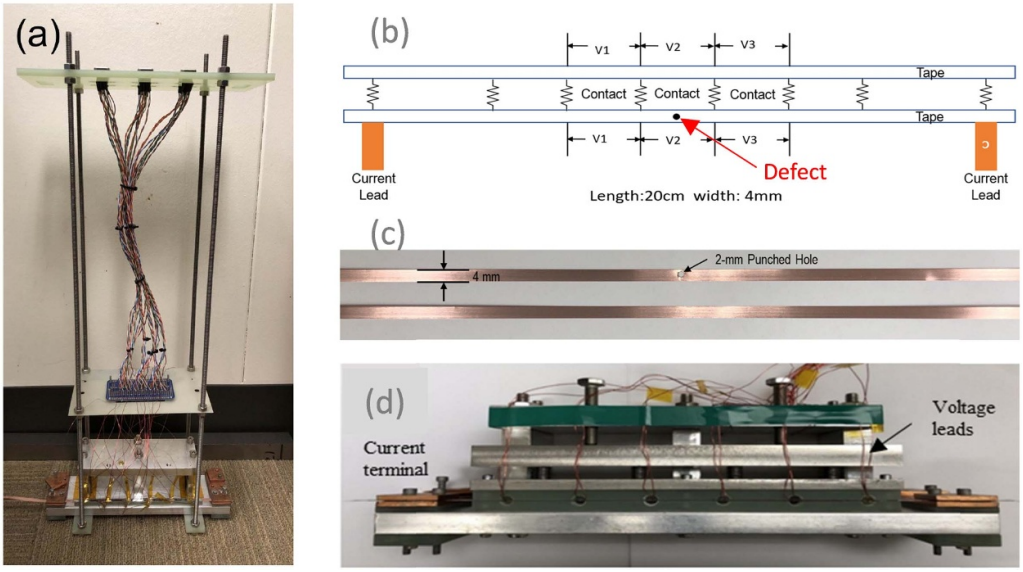

Figure 1. The current sharing experiment: (a) the test rig; (b) schematic of the circuit used showing a defect made in one of the tapes, (c) photograph of two 4 mm wide tapes with one tape with a 2 mm diameter artificial defect (d) photograph of the setup showing current terminals and voltage leads for measurements at multiple tape locations.

tape, a defect was made in one layer, and the defective layer was in contact with the current lead. In a 2-ply stack of double-sided tapes, one layer of one tape consisted of the artificial defect and this layer was in contact with the second double-sided tape that had no artificial defect. Our experimental results showed that when the tapes are in direct contact with the applied pressure, the current distribution is principally determined by the terminal resistance, which is consistent with the reported behavior in studies on REBCO cables [27, 28]. Current flow forced by high or uneven terminal resistance may override and quench the defective strand, and in the worst case, trigger a chain effect that quenches the entire tape stack/cable. We found that current sharing between the two tapes was greatly improved when they were soldered together.

In all 2-ply stacks, the surface oxide on the copper stabilizer was removed by light polishing before the tapes were soldered together. After the tape surface was polished, soldering flux was applied immediately to prevent re-formation of the oxide layer. Then, the contacting surface of each tape was coated with a layer of indium using a solder gun operated at 165 °C or an indium tape was placed on the contacting surface of each tape. Next, the two indium-coated tapes were placed into a compression unit and heat treated at 165 °C for completion of the bonding.

The total length between the two current terminals used for current sharing experiments is ∼25 cm. Due to the unbalanced terminal resistance on two REBCO tapes, the current was introduced into the defective one and shared with the good one in parallel. Once the applied current reaches the local I_c of the defective tape's weakest area, the voltage increases drastically and forces the rest of the current through the normal tape in parallel. A multi-channel data acquisition system monitors the voltage on the central 15 cm length with up to six voltage taps on each REBCO layer. Four or six voltage taps were used in tests to monitor voltages from three or five sections of the tapes, respectively. In the tests, the current was applied to the tape stack at 0.5 A s^{-1} ramping rate, and the voltage signals were monitored using a 28-bit data acquisition system. We adopted an oversampling and averaging technique to ensure that the voltage resolution was better than 0.1 μV.

3. Results and discussion

The current sharing limit of a single tape/layer $\boldsymbol{I_{defect}}$ is the current value on the current–voltage (I–V) curve at which the defective tape/layer becomes non-superconducting based on the 1 μV cm^{-1} voltage criterion. The current sharing limit of the tape stack $\boldsymbol{I_{c,total}}$ is the current value on the I–V curve where the voltage of the parallel tape/layer transitions to a power law behavior. The current sharing behavior in REBCO conductors is determined by the synergetic effect of inter/inner-strand electrical contact resistance, inter-strand thermal contact resistance, boundary cooling condition, and defect density [29]. Hence, in addition to directly measuring the electrical contact resistance, we introduce the **current sharing metric (CSM)** to characterize and quantify the current sharing behaviors in different configurations.

The **CSM** is defined as the ratio of the maximum achieved current to the nominal I_c. For a single-sided tape in a 2-ply stack, i.e. two tapes in contact with each other, the CSM of the defective tape is: $\boldsymbol{CSM_{s-tape,defect}} = \boldsymbol{I_{s-tape,defect}}/\boldsymbol{I_{s-tape-defect,nominal}}$, where $\boldsymbol{I_{s-tape,defect}}$ is the measured critical current of a single-sided tape with a defect and $\boldsymbol{I_{s-tape-defect,nominal}}$ is the nominal critical current of a single-sided tape with a defect. For example, when a defect of 2 mm diameter is introduced in a 4 mm wide single-sided tape with a I_c of 160 A, the nominal I_c of a 4 mm

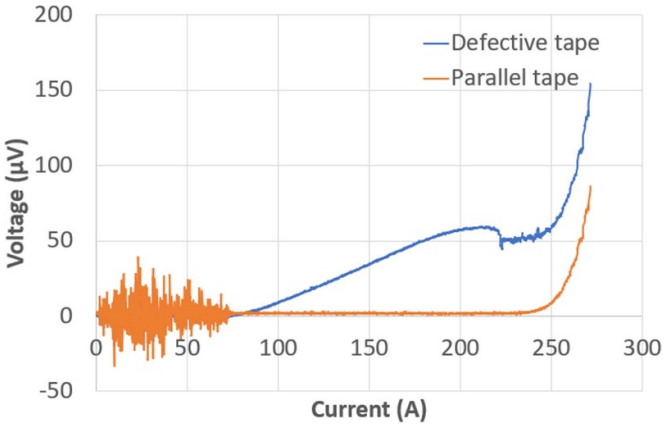

Figure 2. *I–V* curves at 77 K, self-field from the central voltage taps around an artificial defect in one tape and a parallel, normal tape in a 2-ply stack of single-sided tapes soldered with indium in a face-to-back structure.

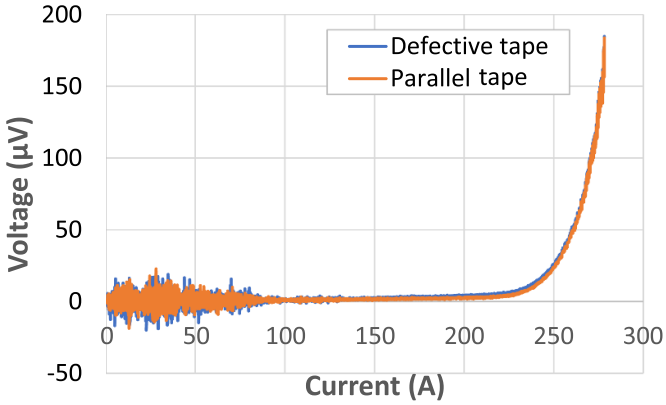

Figure 3. *I–V* curves at 77 K, self-field from the central voltage taps around an artificial defect in one tape and a parallel, normal tape in a 2-ply stack of single-sided tapes soldered with indium in a face-to-face structure.

defective tape is 80 A. If the measured I_c of the defective tape in the 2-ply stack is 90 A, the $\boldsymbol{CSM_{s-tape,\,defect}} = 90/80 = 1.125$. The lowest CSM would be 1 with no current sharing; CSM < 1 would indicate additional damage to the defective tape before experiment. The upper limit of CSM could be $(\boldsymbol{I_{s-tape-parallel,\,nominal}} + \boldsymbol{I_{s-tape-defect,\,nominal}})/\boldsymbol{I_{s-tape-defect,\,nominal}} = (160 + 80)/80 = 3$, with perfect current sharing. Note that the maximum CSM is dependent on the I_c of the good tape in parallel ($\boldsymbol{I_{s-tape-parallel,\,nominal}}$). For a double-sided tape, the CSM of the defective layer is $\boldsymbol{CSM_{d-layer,\,defect}} = \boldsymbol{I_{d-layer,defect}}/\boldsymbol{I_{d-layer,defect,nominal}}$, where $\boldsymbol{I_{d-layer,\,defect}}$ is the measured critical current of the defective layer in a double-sided tape and $\boldsymbol{I_{d-layer,defect,nominal}}$ is the nominal critical current of the defective layer in a double-sided tape.

3.1. Case 1: single-sided tape, 2-ply tape stack, face-to-back structure

Figure 2 shows current sharing in a 2-ply stack of single-sided tapes with a face-to-back structure, soldered with indium. The noise in the voltage data up to ~70 A in the *I–V* curves shown in this figure and other figures of this paper are from the measurement instrumentation. From figure 2, it is seen that the tape stack $I_{c,total}$ is 245 A, and the current sharing limit $\boldsymbol{I_{s-tape,defect}}$ is 82 A. Since the nominal I_c of the defective tape is 80 A, the CSM $\boldsymbol{CSM_{s-tape,\,defect}} = \frac{82}{80} = 1.025$. The tape CSM is just above one, which means by soldering a defective tape to a parallel tape, the defective tape benefits by sustaining a current higher than its nominal I_c. Nevertheless, the improvement is very small—because of the high contact resistivity between the two tapes in a F2B stack configuration as discussed later in figure 4.

A voltage drop can be observed in figure 2 around 220 A in the defective tape followed by a quick voltage increase. This is believed to occur because the cooling capacity of liquid nitrogen has reached its maximum, which is the transition point from nucleation boiling to film boiling [30].

3.2. Case 2: single-sided tape, 2-ply stack, face-to-face structure

Figure 3 exhibits current sharing in a 2-ply stack of single-sided tapes with a face-to-face structure, soldered with indium. Here, the defective tape transitions into a non-superconducting state at essentially the same current as the parallel/normal tape, which indicates perfect current sharing between the two tapes. At a 1 μV cm^{-1} criterion, the transition occurs at 225 A. So, CSM of the F2F configuration = 225/80 = 2.81, which is much higher than the CSM measured for tapes in the F2B configuration.

The much better current sharing between tapes in an F2F configuration than in an F2B configuration is because of the significantly lower contact resistivity in the former as shown in figure 4. The contact resistance between two tapes of different tape stacking configurations, F2F, F2B, and B2B, were compared based on the current–voltage (*I–V*) curves of different soldered joints. Although the tape configurations vary for different joints, each joint consisted of tapes with I_c of 155 A, width of 4 mm, joint overlapping area that is 4 mm wide and 50 mm long and with Sn60Pb40 solder to make the joint. As seen in figure 4, the contact resistivity between tapes in a F2F configuration is more than 20 times lower than that measured in a F2B configuration. A face-to-back contact between REBCO tapes in a tape stack, cable or coil winding is inevitable when using a standard REBCO tape architecture, and the significantly higher contact resistivity in this configuration will limit the extent of current sharing.

3.3. Case 3: double-sided tape, 2-ply tape stack

We also tested current sharing between two stacked, 4 mm wide double-sided REBCO tapes. The two segments of 4 mm wide samples were slit from one 12 mm wide double-sided

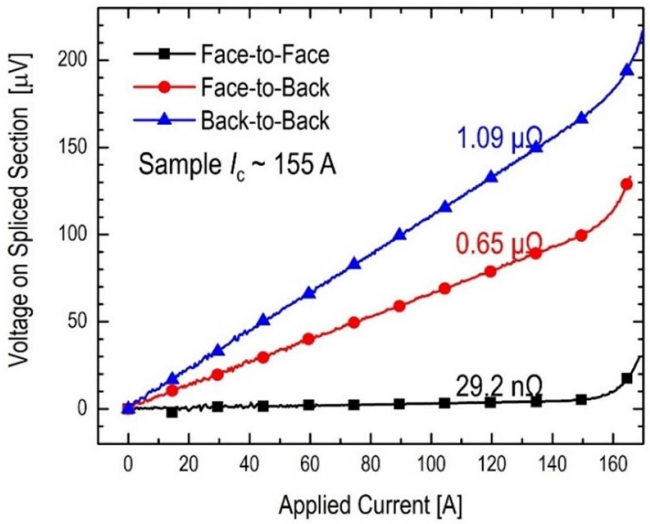

Figure 4. Contact resistivity between two 4 mm wide REBCO tapes plated with 10 μm copper all-around and a 4 $\times$50 mm^2 soldered contact area.

tape prepared by Advanced MOCVD. The samples were checked with reel-to-reel SHPM at 77 K to ensure they were free of major I_c dropouts.

Current sharing between two stacked 4 mm wide double-sided REBCO tapes was tested out with the configuration shown in figure 5. Two double-sided REBCO tapes were stacked with the contacting surfaces soldered together. We attached six voltage taps on each surface of the double-sided REBCO tapes, and all voltage taps were insulated from each other using Kapton. An artificial defect of 2 mm diameter was introduced on the contacting surface of one tape, shown as a red dot in figure 5 (top) and in the photo in figure 5 (middle). Figure 5 (bottom) shows the schematic of the current sharing paths between face-to-face contacts and between the two adjacent layers of double-sided REBCO tapes. The terminals of both double-sided tapes were sheathed with silver to reduce the imbalance of terminal resistance.

Figure 6 shows the *I*–*V* curves obtained from the center (#3) section of the double-sided REBCO tapes: (a) the contact surface of the defective tape where the artificial defect is located; (b) the outer surface of the defective tape; (c) the contact surface of the normal tape; (d) the outer surface of the normal tape. It is confirmed that localized current sharing occurred around the defective section, as plotted in figure 6. The current is well shared between the two contacting surfaces of the defective tape and the normal tape, as they reach the transition and voltage criterion at a similar current (~155 and 160 A), even though the defective tape has a much lower current-carrying capacity due to the artificial defect. The CSM is 1.94. This good current sharing is due to the low face-to-face contact resistivity between the two double-sided tapes.

The outer surfaces reach transition at a higher applied total current (~200 A), indicating that the current sharing between two REBCO layers of each double-sided tape is weaker than the face-to-face contact. This is understandable as the buffer stack is an insulating barrier and the connection between the two sides is only through the silver and copper coating at the edges of the tapes.

3.4. Case 4: one double-sided tape

Since double-sided tapes present the opportunity to share current within one tape itself, from one REBCO layer to the opposite layer, we next explored current sharing within a 4 mm wide double-sided tape, from one layer with a 2 mm diameter artificial defect to the opposite layer with no artificial defect. The 2 mm diameter defect was created in the layer with a higher I_c of 143 A at 77 K, self-field prior to the defect. The nominal I_c of this defective side is now 71.5 A. Transport current was injected into this layer and the results from the current sharing experiment are shown in figure 7. The current sharing limit, $\boldsymbol{I_{s-layer,defect}}$, measured on the defective layer is 106 A. So, the CSM $\boldsymbol{CSM_{s-tape,defect}} = \frac{106}{71.5} = 1.48$. Since the current is injected into the defective layer, it fills this layer first and after it transitions at 106 A, the current flows in the parallel layer without the defect. This parallel layer without the defect transitions is now at a much higher current of 190 A, well beyond the nominal I_c of this layer.

3.5. Laser slotting to reduce contact resistivity between two REBCO layers within a double-sided tape

In order to promote current sharing between two layers of a double-sided tape (Case 4) and between two single-sided tapes in a 2-ply stack (Case 1), we are developing methods to reduce contact resistivity, including, electrically-conductive buffer layers; and laser slotting to remove small portions of the insulating buffer stack and filling the slots with a conductive material. In the latter architecture, the slots filled with conductive material will connect the REBCO layer to the substrate. Results on laser-slotted tapes to promote current sharing between the two REBCO layers of double-sided tapes will be discussed in this paper. Other results will be reported elsewhere.

To guide our work on laser slotting, we developed a 2D finite element analysis (FEA) model, to analyze the current flow between two tapes in contact with each other. A similar numerical method has been validated to have an acceptable accuracy [31]. We calibrated the model by matching the numerical and measurement results in a parametric sweep study.

Different numbers of slots are introduced across the width of the tape. Figure 8(a) shows a cross sectional view of a double-sided tape where two slots are created on each side of the tape across the tape width direction and positioned identically along the tape length. In addition, the two slots on one side are aligned with their counterparts on the other side of the tape in the tape thickness direction. In the FEA model, the width of each slot was fixed at 0.1 mm and the depth was varied. The

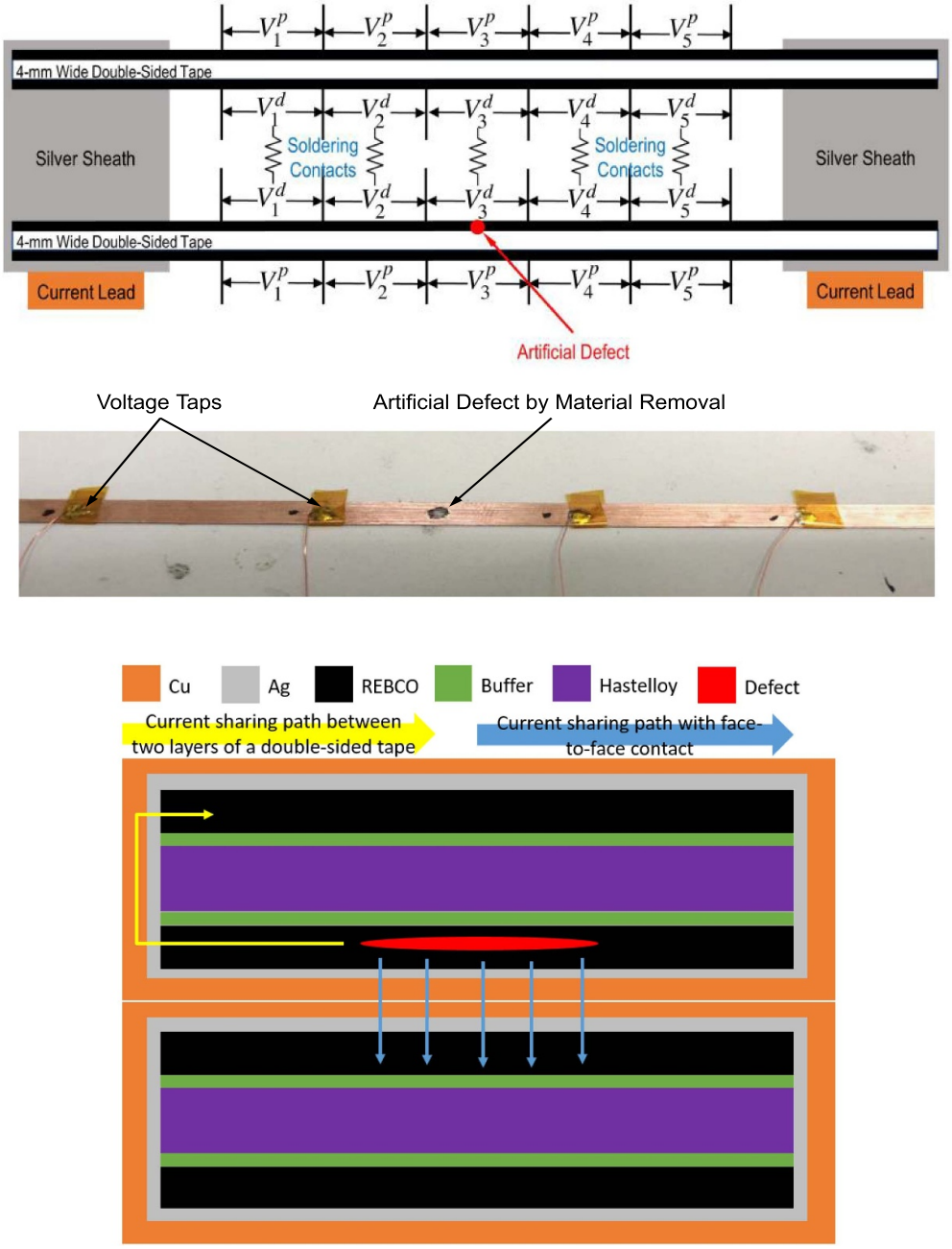

Figure 5. (Top) Stacking configuration of two double-sided REBCO tapes for current sharing tests. (Middle) A 4 mm wide double-sided tape with an artificial defect of 2 mm diameter introduced on the contacting surface of one tape. (Bottom) Current sharing path in two double-sided tapes.

slots were considered to be filled with Ag which has an electrical conductivity of 2.7 nΩm at 77 K [32]. Figure 8(b) shows that creating slots on only one side will not result in a reduction in current sharing resistance because of the absence of a low resistivity path through the insulating buffer layer on the other side. However, as figure 8(b) reveals, current sharing resistance within one double-sided REBCO tape can be reduced by cutting slot patterns on both sides and filling the slots with an electrically-conductive material. The resistance decreases as the number of slots increases. Figure 8(c) presents the relationship between the current sharing resistance in a double-sided tape and the depth of slot into the Hastelloy substrate. As the depth increases, more Hastelloy is replaced with silver, which is a better conductor, and therefore the current sharing resistance decreases. The trend for '0 μm' also shows a decrease in the current sharing resistance as the number of slots increases, because, even though the slots do not cut into the Hastelloy, the insulating buffer layer is removed.

We prepared slotted REBCO tape with a reel-to-reel laser slitting tool to create narrow slots that penetrate both REBCO and buffer layers. The reel-to-reel laser system was program controlled to customize the slotting pattern on the

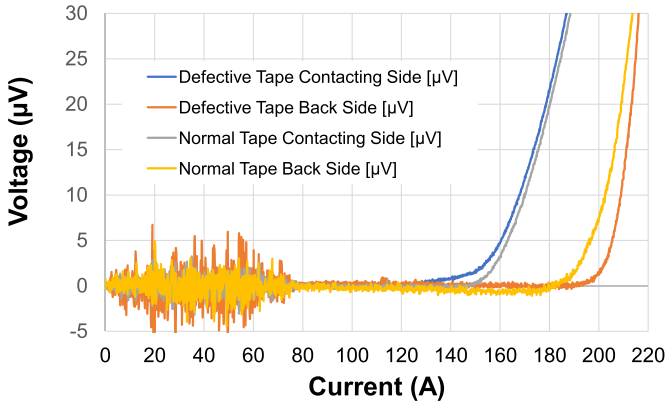

Figure 6. *I–V* curves at 77 K, self-field from the central section of the 2-stack double-sided tapes. An artificial defect is located at the center section S3 on the contacting surface of the defective tape. Nearly equal current distribution in seen in both tapes, indicative of excellent current sharing to bypass the artificial defect.

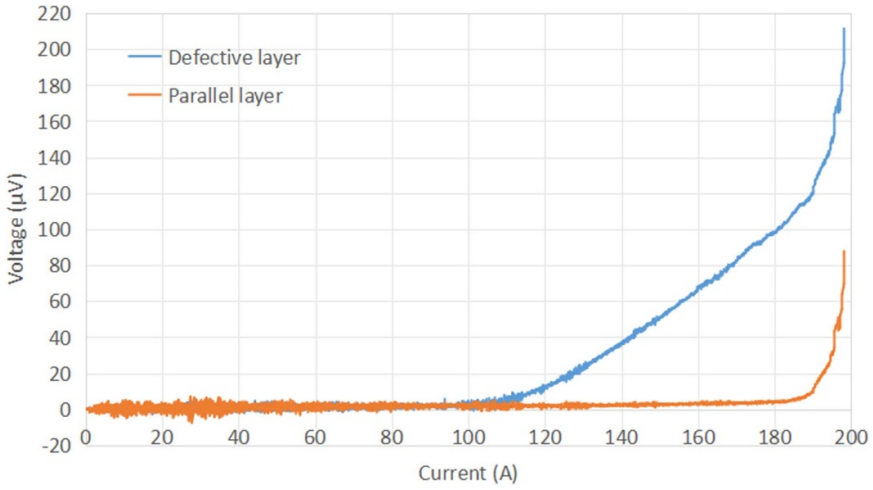

Figure 7. *I–V* curves at 77 K, self-field from the two REBCO layers on opposite sides of a 4 mm wide double-sided tape. An artificial defect of 2 mm diameter was made on one layer of the tape.

REBCO tape. Because a complete striation over the entire tape length may introduce additional current sharing issues between filaments, we prepared slots in dash-line form which will not disrupt the overall continuity of REBCO film. A 2–2 slotting pattern is shown in figure 9. 2–2 refers to two slots across the tape width direction at the same position along the tape length. We first slotted the 12 mm original tape on the REBCO film side, and then laser slit it from the substrate side into 3 segments of 4 mm wide tapes. Each slot has a width of 0.1 mm and a length of 0.5 mm; the distance between two slots is 1.2 mm across tape width and 0.5 mm along tape length.

The width of the slots was chosen to allow >90% of the superconducting paths to remain across the tape width (y-axis) after slotting. The length and spacing of the slots were chosen to maximize the conductive path through the slots while preserving at least 50% of REBCO along the length of the tape at the y-axis position where the slots were created. The y-axis position of the slots was chosen to be at the ¼ of tape width. Because all the critical current data we report in this work are at self-field, it will not matter much if the slots are created at the center or near the edge of the tape. If the tapes are measured under a background field or an AC field, the edges of the tapes will be subjected to a higher magnetic flux density, leading to lower I_c. Hence, creating slots near the tape edge where the I_c is lower, while maintaining the integrity of the middle high I_c region will be beneficial for I_c preservation. However, in magnets, there will be a twisting force on the tapes due to the screening current [33–35]. In this case, having slots near the edge will increase the susceptibility of the tape to damage. Therefore, in real applications, determining the slot position requires consideration of both I_c preservation and mechanical stability.

In double-sided tapes, the slots were cut on both layers. Silver was then deposited on the slotted REBCO tape to connect the edges of each REBCO filament with the exposed substrate. The tape was further stabilized with ∼10 μm copper plating on each side.

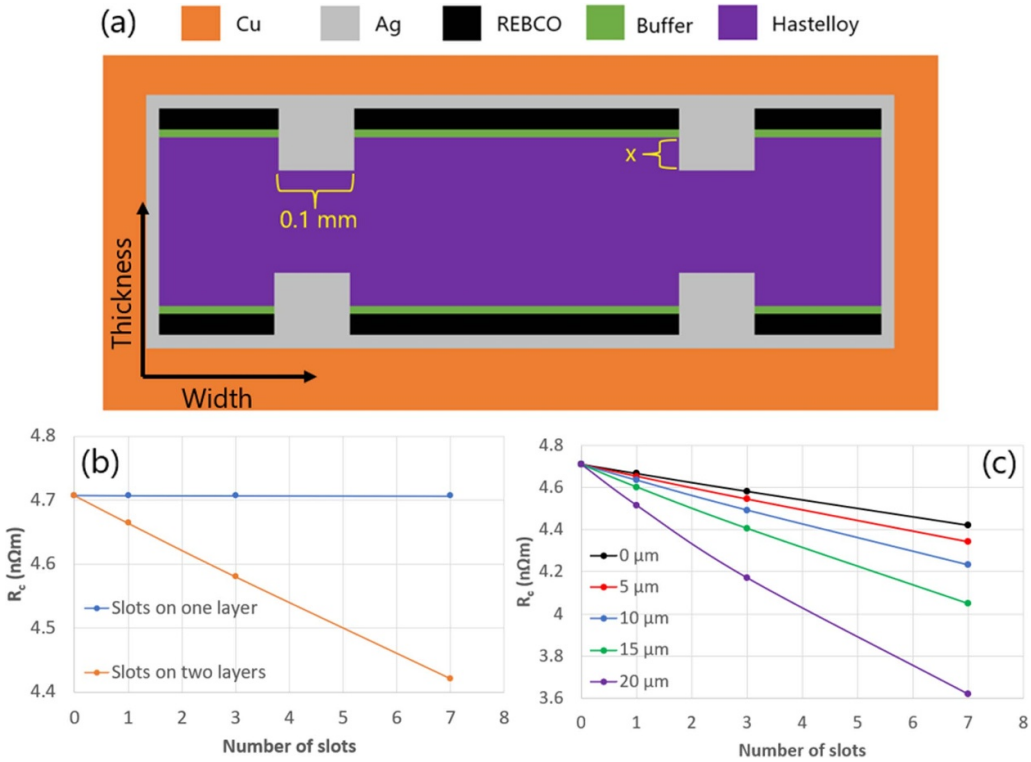

Figure 8. (a) Cross-sectional schematic of double-sided REBCO tape with slots cut into it. (b) Simulation data showing current sharing resistance (R_c) in a double-sided tape with number of slots in one layer and both layers. (c) Current sharing resistance in double-sided tape with slots of different depths into the Hastelloy in both layers.

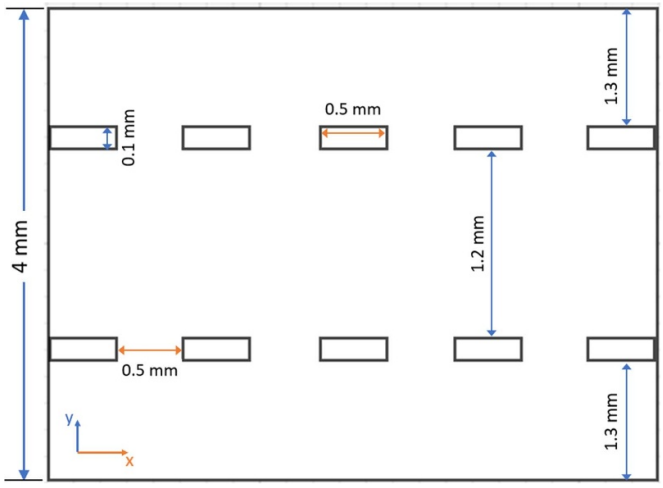

Figure 9. 2–2 laser slot pattern in a REBCO tape. (*X*-direction is the tape length direction, *y*-direction is the tape width direction. Slot features are enlarged for presentation).

3.6. Case 5: double-sided tape with 2–2 slot patterns on both sides

A double-sided tape with slots on both layers in a 2–2 pattern was used for current sharing experiments. The critical current of the tape was reduced by only 7% after slotting, which matches the expected value based on the material removed. This indicates that the laser slotting process does not damage the tape beyond the amount of REBCO film removed. A 2 mm diameter defect was created in the REBCO layer that exhibited a higher I_c after slotting. The nominal I_c of this layer after this defect creation was 105 A. Figure 10 shows the current sharing behavior in this double-sided tape when the current is injected into the defective layer. The current sharing limit seen in figure 10, $\boldsymbol{I_{d-layer,\,defect}} = 175$ A. So, the CSM within the slotted double-sided tape is $\boldsymbol{CSM_{d-layer,\,defect}} = \frac{175}{105} = 1.67$. This value is 13% higher than that observed in Case 4 i.e. current sharing within one double-sided tape with no slots and 67% higher than that obtained in Case 1 i.e. current sharing between two single-sided tapes in face-to-back contact. This result confirms the effectiveness of the slotting method to enhance current sharing between the two layers of one double-sided tape. It can be observed that the *I*–*V* curve of the parallel layer has a slope after 175 A. We believe that this slope is the result of the heating effect from the current shared by the defective layer after it reaches its I_c. Data showing the benefit of slotting to improve current sharing between single-sided REBCO tapes in face-to-back contact will be presented in a future publication.

Figure 11 exhibits data from another current sharing experiment in a similar slotted double-sided tape. In this case, a 2 mm diameter defect was created in the layer that exhibited a lower I_c after slotting. The nominal I_c of this layer after defect creation was 57 A. The current sharing limit seen in figure 11, $\boldsymbol{I_{d-layer,\,defect}} = 108$ A. So, the CSM within the slotted double-sided tape is $\boldsymbol{CSM_{d-layer,defect}} = \frac{108}{57} = 1.89$. Regardless of whether the defect is created in the lower or higher I_c layer, it is seen that slotting enhances

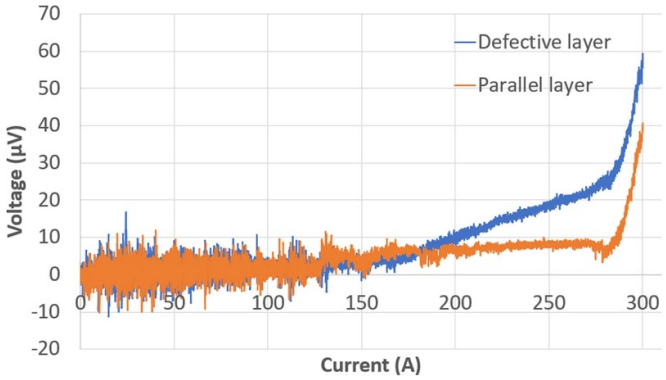

Figure 10. *I–V* curves at 77 K, self-field from the two REBCO layers on opposite sides of a 4 mm wide double-sided tape with slots cuts in a 2–2 pattern on both sides. Current is injected into the defective layer that has a 2 mm artificial defect.

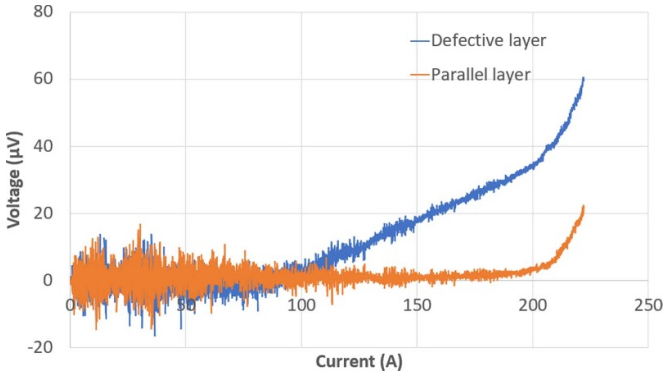

Figure 11. *I–V* curves at 77 K, self-field from the two REBCO layers on opposite sides of a 4 mm wide double-sided tape with slots cut in a 2–2 pattern on both sides. Current is injected into the defective layer that has a 2 mm artificial defect.

Table 1. Comparison of current sharing metric of five different tape configurations investigated in this work.

Case	Contact configuration	Defective tape I_c (A)	Current sharing I_c (A)	CSM
1	Single-sided tapes: face-to-back (F2B)	80	82	1.03
2	Single-sided tapes: face-to-face (F2F)	80	225	2.81
3	Two double-sided tapes	80	155	1.94
4	Within one double-sided tape	106	71.5	1.48
5	Within one double-sided tape with 2–2 slot	105	175	1.67
	patterns on both REBCO layers	57	108	1.89

current sharing between the two layers of a double-sided tape.

4. Summary

Current sharing between single-sided REBCO tapes and between double-sided REBCO tapes in a 2-ply stack as well as between the two REBCO layers within one double-sided tape has been investigated. Current sharing experiments were conducted with 4 mm wide tapes with a 2 mm diameter defect created in one of the tapes in a 2-ply stack or in one of the REBCO layers of a double-sided tape. A CSM, defined as the ratio of the measured critical current of the tape or layer with the artificial defect compared to the nominal critical current of the defective tape/layer, has been used to compare the current sharing efficacy of different tape architectures studied in this work. Table 1 summarizes the experimental results and compares the CSM of the investigated tape configurations.

As expected, in a 2-ply stack of single-sided tapes, the face-to-face configuration yielded a much higher CSM than the face-to-back configuration. In a 2-ply stack of double-sided tapes, the contacting surfaces (one with an artificial defect) show nearly equal current sharing because of the face-to-face configuration always available with double-sided tapes. The CSM between the two REBCO layers of one double-sided tape was, however, low, presumably because of the insulating buffer stack intervening between the two REBCO layers. A laser slotting technique, wherein narrow slots are introduced through the REBCO film and buffer stack followed by fill up of the slots with silver, has been developed to reduce the current sharing resistivity between the two REBCO layers within

a double-sided tape. Simulation data showed that the current sharing resistivity decreased more with the number of slots when the slots are introduced on both sides of the tape and with deeper slots. Regardless of whether the artificial defect was created in a higher I_c or lower I_c layer of a double-sided tape, a high CSM was achieved in the current transfer between the defective layer and normal layer of slotted double-sided tapes. Defect-tolerant tapes such as those demonstrated in this work will be extremely beneficial in avoiding potential damage with uncontrolled quench in REBCO tapes where high currents are sustained through films just 2–5 μm thick.

Data availability statement

All data that support the findings of this study are included within the article (and any supplementary files).

Acknowledgments

This work was supported by the U.S. Naval Sea Systems Command Small Business Technology Transfer Awards N68335-21-C-0525 and N68335-23-C-0228 and the Advanced Research Project Agency—Energy (ARPA-E) Award DE-AR0001374. One author (VS) has financial interest in AMPeers LLC.

ORCID iDs

Yi Li https://orcid.org/0000-0001-8009-6329
Venkat Selvamanickam https://orcid.org/0000-0001-6618-9406

References

[1] Wulff A C, Abrahamsen A B and Insinga A R 2021 *Supercond. Sci. Technol.* **34** 053003
[2] Wang X, Caspi S, Dietderich D R, Ghiorso W B, Gourlay S A, Higley H C, Lin A, Prestemon S O, van der Laan D and Weiss J D 2018 *Supercond. Sci. Technol.* **31** 045007
[3] Liu S, Ren L, Li J and Tang Y 2011 *Physica* C **471** 1080–2
[4] Chen H, Liu H J, Liu F and Shi Y 2021 *IEEE Trans. Appl. Supercond.* **31** 9001004
[5] van Nugteren J, Dhalle M, Wessel D, Krooshoop E, Nijhuis A and ten Kate H 2015 *Phys. Proc.* **67** 945
[6] Bellis R H and Iwasa Y 1994 *Cryogenics* **34** 129
[7] Dixit M, Kim T H, Kim H M, Song K J, Oh S S, Ko R K, Kim H S and Park K B 2006 *Physica* C **434** 199
[8] Haro E, Jarvela J and Stenvall A 2015 *J. Supercond. Nov. Magn.* **28** 1705
[9] Ishiyama A, Ueda H, Aoki Y, Shikimachi K, Hirano N and Nagaya S 2011 *IEEE Trans. Appl. Supercond.* **21** 2398
[10] Wang X R, Caruso A R, Breschi M, Zhang G, Trociewitz U P, Weijers H W and Schwartz J 2005 *IEEE Trans. Appl. Supercond.* **15** 2586
[11] Abraimov D *et al* Review of Ic variation, Rc, RRR and other parameters *WAMHTS-1* (21–23 May 2014)
[12] Li Y *et al* 2022 *IEEE Trans. Appl. Supercond.* **32** 9000206
[13] Kovacs C J, Sumption M D, Majoros M and Collings E W 2020 *IEEE Trans. Appl. Supercond.* **30** 6600505
[14] Bonura M, Barth C, Joudrier A, Troitino J F, Fete A and Senatore C 2019 *IEEE Trans. Appl. Supercond.* **29** 6600305
[15] Lu J, Goddard R, Han K and Hahn S 2019 *Supercond. Sci. Technol.* **30** 045005
[16] Xue S, Sumption M D and Eward C 2021 *IEEE Trans. Appl. Supercond.* **31** 7000305
[17] Xue S 2022 *IEEE Trans. Appl. Supercond.* **32** 4802506
[18] Shin H S, Nisay A, de Leon M B and Dedicatoria M J 2015 *IEEE Trans. Appl. Supercond.* **25** 6602205
[19] Shin H S, Diaz M A, Bautista Z M and Awaji S 2018 *IEEE Trans. Appl. Supercond.* **28** 6600405
[20] Xue S 2023 *PhD Thesis* Ohio State University
[21] Lee W, Park D, Bascunan J and Iwasa Y 2022 *Supercond. Sci. Technol.* **35** 105007
[22] Hartwig Z S *et al* 2020 *Supercond. Sci. Technol.* **33** 11LT01
[23] Hartwig Z S *et al* 2023 *IEEE Trans. Appl. Supercond.* **34** 0600316
[24] Paidpilli M, Sandra J S, Sarangi B, Goel C, Galstyan E, Majkic G and Selvamanickam V 2023 *Supercond. Sci. Technol.* **36** 095016
[25] Li X-F *et al* 2017 *IEEE Trans. Appl. Supercond.* **27** 7792641
[26] Chen S, Li X-F, Luo W and Selvamanickam V 2019 *IEEE Trans. Appl. Supercond.* **29** 6601504
[27] Willering G P, van der Laan D C, Weijers H W, Noyes P D, Miller G E and Viouchkov Y 2015 *Supercond. Sci. Technol.* **28** 035001
[28] Michael P C, Bromberg L, van der Laan D C, Noyes P and Weijers H W 2016 *Supercond. Sci. Technol.* **29** 045003
[29] Xue S *et al* 2023 *IEEE Trans. Appl. Supercond.* **33** 4801107
[30] Berger A D 2012 MIT plasma science and fusion center *Technical Report* (available at: http://hdl.handle.net/1721.1/93343)
[31] Park D K, Ahn M C, Kim H M, Lee H G, Sung Chang K I, Jin Lee S, Eun Yang S and Kuk Ko T 2007 *IEEE Trans. Appl. Supercond.* **17** 3266
[32] Smith D R and Fickett F R 1995 *J. Res. Natl Inst. Stand. Technol.* **100** 158
[33] Yan Y, Li Y and Qu T 2022 *Supercond. Sci. Technol.* **35** 014003
[34] Suetomi Y, Xu P, Bosque E S, Gavrilin A V, Markiewicz W D, Bai H and Dixon I R 2024 *IEEE Trans. Appl. Supercond.* **34** 8400206
[35] Ueda H, Maeda H, Suetomi Y and Yanagisawa Y 2022 *Supercond. Sci. Technol.* **35** 054001